


Quality Amplification of Error Prone Navigation for Swarms of Micro Aerial Vehicles (with Detailed Simulations)

Michel Barbeau
Carleton University, Canada
 0000-0003-3531-4926

Joaquin Garcia-Alfaro
Telecom SudParis, France
 0000-0002-7453-4393

Evangelos Kranakis
Carleton University, Canada
 0000-0002-8959-4428

Fillipe Santos
University of Campinas, Brazil
 0000-0002-3698-2304

Abstract—We present an error tolerant path planning algorithm for Micro Aerial Vehicle (MAV) swarms. We assume a MAV navigation system without relying on GPS-like techniques. The Micro Aerial Vehicles (MAVs) find their navigation path by using their sensors and cameras, in order to identify and follow a series of visual landmarks. The visual landmarks lead the MAVs towards the target destination. MAVs are assumed to be unaware of the terrain and locations of the landmarks. Landmarks are also assumed to hold a-priori information, whose interpretation (by the MAVs) is prone to errors. We distinguish two types of errors, namely, *recognition* and *advice*. Recognition errors are due to misinterpretation of sensed data and a-priori information or confusion of objects (e.g., due to faulty sensors). Advice errors are due to outdated or wrong information associated to the landmarks (e.g., due to weather conditions). Our path planning algorithm proposes swarm cooperation. MAVs communicate and exchange information wirelessly, to minimize the *recognition* and *advice* error ratios. By doing this, the navigation system experiences a quality amplification in terms of error reduction. As a result, our solution successfully provides an adaptive error tolerant navigation system. Quality amplification is parametrized with regard to the number of MAVs. We validate our approach with theoretical proofs and numeric simulations.

I. INTRODUCTION

MAVs are a popular type of drones. They are equipped with sensors and cameras, making it possible to hover and navigate complex three dimensional terrains. They may be used in a variety of applications, including sewer inspection [1], search and rescue operations [2], and parcel delivery [3]. Large terrains can be covered by so called swarms, namely collaborative teams of MAVs, which may exchange information gathered during navigation and as such may become resilient to potential MAV failures of all kinds either in navigation or sensitivity of sensor equipment. We are interested in designing swarm algorithms that are resilient to such random failures.

We present an error tolerant path planning algorithm for MAV swarms. We assume a MAV navigation system without relying on GPS-like techniques. MAVs find their navigation path by using their sensors and downward cameras, in order to identify and follow a series of visual landmarks. The visual landmarks lead the MAVs towards the target destination. We assume that the MAVs are unaware of the terrain and locations of the landmarks. Figure 1 shows the idea. A swarm of MAVs collectively identify a series of landmarks over an inspected terrain. The identification of the landmarks allows the swarm to find the path that the MAVs must follow.

To address the path finding problem, the swarm considers a terrain comprising a set of multiple waypoints or landmarks. The landmarks also include the starting and terminal points of a well-defined path. The MAVs may hover over the landmarks either on their own or in formation. They may hop from anyone landmark to any other. The landmarks are identified as vertices and the resulting communication system forms a complete graph. Recall that the MAVs are unaware of the terrain and locations of the landmarks. However, they have the capability to visually recognize the landmarks. Further, the MAVs may communicate and exchange information wirelessly as long as they are within communication range of each other. The MAVs are required to find a flight path from the starting point, leading to the terminal point.

We also assume that the landmarks hold information whose interpretation (by the MAVs) is prone to errors. We distinguish two types of errors, namely, *recognition* and *advice*. Recognition errors are due to misinterpretation of sensed data and a-priori information or confusion of objects (e.g., due to faulty sensors). Advice errors are due to outdated or wrong information associated to the landmark (e.g., due to weather conditions). Our path planning algorithm is based on swarm cooperation. MAVs may communicate and exchange information wirelessly, in order to minimize the *recognition* and *advice* error ratios. In other words, by collaboratively exchanging information, the swarm of MAVs experiences a *quality amplification*, in terms of error reduction. As a result, the swarm gets equipped with an adaptive error tolerant navigation mechanisms, in which quality gets parameterized with regard to the number of MAVs.

We show how our approach improves the probability of navigation correctness when the number of MAVs in the swarm increases, i.e., when the wireless communica-



Fig. 1. Sample picture taken from an aerial vehicle, together with the identification of six landmarks at the campus of Carleton University.

tion among MAVs allows them to cooperatively exchange information about the landmarks. The idea is as follows. When the swarm contains only a single MAV, *recognition* and *advice* errors directly affect the whole navigation system. The MAV can get disrupted by such errors, and get lost forever. When the number of MAVs in the swarm increases, communication and exchange of information between MAVs takes place. The quality of the merged data increases as well. We analyze the reduction in the error probability induced by our algorithmic solutions, and experimentally validate the results via numeric simulations. Hence, quality amplification is demonstrated both analytically and experimentally.

Section II surveys related work. Sections III and IV present our proposal. Section V evaluates the work. Section VI concludes the paper. Appendix A provides additional information about experimental work.

II. RELATED WORK

Surveys on path planning algorithms for unmanned aerial vehicles have been authored by Goerzen et al. [4] and Radmanesh et al. [5]. Several algorithms build on solutions originally created for computer networks. Some of the proposed solutions leverage algorithms created in the field of classical robotics, such as approaches using artificial potential functions [6], random trees [7] or Voronoi diagrams [8]. Path planning may be addressed in conjunction with team work and formation control [9]. There are ideas that have been tailored specifically to quadcopters [10].

Our research is closely related to works on navigation using topological maps [11]. Navigation does not rely on coordinates. The MAVs find their way recognizing landmarks. Weinstein et al. [12] propose the use of visual odometry as an alternative localization technique to, e.g., GPS-like techniques. The idea is as follows. The MAVs use their onboard cameras (e.g., downward facing cameras), combined by some inertial sensors, to identify and follow a series of visual landmarks. The visual landmarks lead the MAV towards the target destination. Unlike GPS, the technique allows the MAV to operate without boundaries in both indoor and outdoor environments. No precise information about concrete visual odometry techniques are reported by Weinstein et al. in their work. However, some ideas can be found in [13], [11].

Maravall et al. [13], [11] propose the use of probabilistic knowledge-based classification and learning automata for the automatic recognition of patterns associated to the visual landmarks that must be identified by the MAVs. A series of classification rules in their conjunctive normal form (CNF) are associated to a series of probability weights that are adapted dynamically using supervised reinforcement learning [14]. The adaptation process is conducted using a two-stage learning procedure. During the first process, a series of variables are associated to each rule. For instance, the variables associated to the construction of a landmark recognition classifier are constructed using images' histogram features, such as standard deviation, skewness, kurtosis, uniformity

and entropy. During the second process, a series of weights are associated to every variable. Weights are obtained by applying a reinforcement algorithm, i.e., incremental R-L algorithm in [14], [11], over a random environment. As a result, the authors obtain a specific image classifier for the recognition of landmarks, which is then loaded to the MAVs.

The resulting classifiers had been tested via experimental work. MAVs with high-definition cameras, recording images at a resolution of 640x360 pixels, at the speed of 30 fps (frames per second) are loaded a given classifier, to evaluate a visual classification ratio. Each experiment consists of building a classifier and getting the averaged ratio. Results by Maravall et al. in [13], [15] show an average empirical visual error ratio of about 20% (i.e., 80% chances of properly identifying the landmarks, on average). The results are compared to some other well-established pattern recognition methods for the visual identification of objects, such as minimum distance and k -nearest neighbor classification algorithms.

The previous contribution is complemented by Fuentes et al. and Maravall et al. in [16], [11], by combining the probabilistic knowledge-based classifiers with bug algorithms [8], to provide the MAVs with a navigation technique to traverse a visual topological map composed of several visual landmarks. A technique is used to compute the entropy of the images captured by the MAV, in case a decision must be taken (e.g., to decide whether going south or north directions). The idea is as follows. The MAV uses the camera onboard, and takes images about several directions. Afterward, it processes the images to chose a given direction. The lower the entropy of a captured image, the lower the probability of going towards an area containing visual landmarks. Conversely, the higher the entropy of a captured image, the higher the probability of going towards an area surrounded by landmarks. Using this heuristic, the MAV collects candidate images with maximum entropy (e.g., by driving the MAV forward and backward some meters) prior executing a bug algorithm to locate the landmarks [11].

The use of the entropy technique in [16], [11] can also be used before processing the images with the visual recognition classifier, to reduce the computational cost (i.e., by processing only those images with high entropy, the MAV can avoid that a costly classifier processes images with low likelihood of containing landmarks).

Our proposed search algorithms resemble graph search with advice and the reader is referred to [17] for related work on the ring and to [18] for complete networks.

III. ERROR PRONE NAVIGATION

We identify the landmarks with the n vertices of a complete graph $G = (V, E)$. Starting at s and ending at t , the MAVs are seeking a flight path connecting $k + 1$ vertices

$$s := v_0, v_1, \dots, v_i, v_{i+1}, \dots, v_k := t$$

where $v_0, v_1, \dots, v_i, v_{i+1}, \dots, v_k$ are in V , see Figure 2. The MAVs have to navigate and find a flight path from s to t using clues. When hovering over an area, a MAV acquires data

through its camera and other sensors, which may be visual, acoustic, etc. This data is used for landmark searching. A priori, the MAVs are given clues and specific characteristics about the landmarks. For example, the MAVs may be seeking a green door or a tall building.

The landmarks provided have a-priori information whose interpretation (by the MAVs) is prone to errors. We distinguish two types of errors, namely, *recognition* and *advice*. Recognition errors are due to misinterpretation of sensed data and a-priori information or confusion of objects. For example, a MAV has found a green door which in fact is not a door but rather a window. The recognized object is incorrect. We assume that for some real number p in the interval $[0, 1]$, the value p is the probability that a MAV performs recognition erroneously and $1 - p$ that it is correct.

Advice errors about landmarks occur because the information provided is not up to date or even wrong. For example, upon finding a landmark a MAV is advised to traverse a certain distance within the terrain in direction north where it will find the next landmark, say a restaurant, but this information is wrong because the restaurant is no longer there. We assume that for some real number q in the interval $[0, 1]$, the value q is the probability that the advice provided to a MAV about a landmark is invalid or erroneously interpreted and $1 - q$ that it is valid and correctly interpreted.

Recognition and advice errors are independent of each other. An important point to be made is that we assume that recognition and advice are random processes. For all MAVs, we make the assumption that recognition errors are independent and identically distributed and advice errors are also independent and identically distributed. The MAVs act independently of each other. Moreover, the outcome of the recognition process is random with probability of success that depends on the parameter p . A similar observation applies to the advice process. As a consequence, we can use this to our advantage so as to improve the recognition and advice mechanisms for swarms of MAVs.

Assume a MAV is navigating the terrain through a flight path, denoted as P , consisting of k vertices $v_0 := s, v_1, \dots, v_i, v_{i+1}, \dots, v_k := t$ from s to t . An edge $\{v_i, v_{i+1}\}$ corresponding to a segment of flight path P is said to be correctly traversed if and only if the advice provided about the landmark associated with vertex v_i is valid and correctly interpreted and the landmark associated with vertex

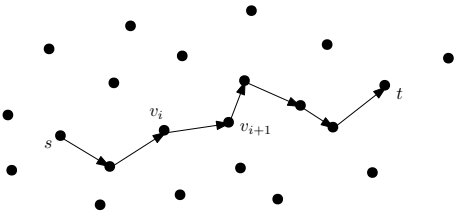


Fig. 2. Flight path from source s to destination t . Edge (v_i, v_{i+1}) is an intermediate segment connecting landmarks v_i and v_{i+1} .

v_{i+1} is correctly recognized. For $i = 0, \dots, k - 1$, the flight path P is correctly traversed if and only if each of its segment defined by an edge $\{v_i, v_{i+1}\}$ is correctly traversed.

At the start, a MAV is given a flight plan. The flight plan defines the flight path P . For each vertex $v_i, i = 0, \dots, k - 1$, the flight plan comprises advice for searching the next landmark, such as directional data. For each vertex v_{i+1} , the flight plan contains recognition data, such as landmark characteristics. A flight plan is correctly performed solely if every single segment is correctly traversed.

We obtain the following quantitative characterization of segment correctness and flight path in terms of recognition and advice probabilities.

Lemma III.1. *A flight plan leading to a path of length k is correctly performed with probability $(1 - p)^k(1 - q)^k$.*

Proof. For individual segments $i = 0, \dots, k - 1$, we have

$$\Pr[\{v_i, v_{i+1}\} \text{ is correct}] = \Pr[\text{advice at } v_i \text{ and recognition at } v_{i+1} \text{ are correct}] = (1 - p)(1 - q).$$

For the whole flight plan for path P , we have

$$\begin{aligned} \Pr[P \text{ is correct}] &= \Pr[\forall i (\{v_i, v_{i+1}\} \text{ is correct})] \\ &= \prod_{i=0}^{k-1} \Pr[\{v_i, v_{i+1}\} \text{ is correct}] \\ &= (1 - p)^k(1 - q)^k. \end{aligned}$$

This proves the lemma. \square

Lemma III.1 is valid for a single MAV that is recognizing landmarks and navigating from a start point to a terminal point. In Section IV it is shown how to improve the probability of correctness for a swarm of co-operating MAVs that communicate and exchange information with each other.

Algorithm 1 Majority Recognition Algorithm for a swarm of m MAVs

- 1: Each MAV performs landmark recognition
 - 2: MAVs exchange information
 - 3: **if** there is a landmark common to the majority (of at least $\lceil m/2 \rceil$ MAVs) **then**
 - 4: the MAV swarm adopts this common landmark
 - 5: **else**
 - 6: every MAV adopts its own recognized landmark
-

Algorithm 2 Majority Advice Algorithm for a swarm of m MAVs

- 1: Each MAV takes the advice provided for the visited landmark
 - 2: MAVs exchange information
 - 3: **if** there is a majority advice interpretation (for at least $\lceil m/2 \rceil$ MAVs) **then**
 - 4: all MAVs follow this common advice interpretation
 - 5: **else**
 - 6: the MAVs follow their own advice interpretation
-

In a swarm, we may take advantage of communications and collaboration among the MAVs so as to amplify the quality of a-priori and sensed data. To this end, we use the principle of maximum likelihood.

Algorithms 1 and 2 define the main processes. Algorithm 1 applies majority recognition. Algorithm 2 applies the advice. It should be emphasized that the amplification of recognition and advice, implied by the majority rule used in the two algorithms above, is based on a binary decision. To illustrate this fact, consider the case of amplification of the quality of recognition. First of all, it is assumed that all the MAVs in the swarm run the same visual recognition software. Hence, the set of possible outcomes of the MAVs' visual systems is partitioned into two mutually disjoint sets. The first set can be interpreted as the container of positive outcomes. The second set as the container of negative outcomes. This is to be the same for all the MAVs. For a binary decision example, consider a swarm of five MAVs which is to decide whether the object viewed is either a Door (D) or a Window (W). If the answers of the individual MAVs are D, W, D, W, D, then the majority output will be Door.

A similar interpretation is being used for the advice algorithm software which is executed by "smart landmarks" giving advice to the MAVs, i.e., providing the direction the swarm should follow next. For a binary example with a swarm of five MAVs, assume that the landmarks may give either the answer North (N) or South (S). If the advice collected by the MAVs are N, S, S, N, N, then the majority decision will be North.

IV. QUALITY AMPLIFICATION AND ERROR REDUCTION

A. Reducing the error probability

The collaborative landmark recognition process defined by Algorithm 1 applies to a swarm composed of m MAVs. Let p_m denote the error probability of the majority rule applied in Algorithm 1; this is given by the following formula.

$$p_m = 1 - \sum_{i=\lceil m/2 \rceil}^m \binom{m}{i} (1-p)^i p^{m-i} \quad (1)$$

Now we show that the majority rule improves the error probability p .

Lemma IV.1. *For $p < 1/2$, we have the following inequality*

$$1 - p < p^m \sum_{i=\lceil m/2 \rceil}^m \binom{m}{i} \left(\frac{1}{p} - 1\right)^i. \quad (2)$$

Proof. (Lemma IV.1) The inequality is proved by considering two cases depending on the parity of m , the number of MAVs.

Case 1: m is odd. If m is odd, we can express the value as $m = 2d + 1$, for some integer $d \geq 1$ so that $\lceil m/2 \rceil = d + 1$.

Let $a = \frac{1}{p} - 1$ and observe that $a > 1$, since $p < \frac{1}{2}$. From the binomial theorem we have that

$$\begin{aligned} (a+1)^m &= \sum_{i=0}^m \binom{m}{i} a^i \\ &= \sum_{i=0}^d \binom{m}{i} a^i + \sum_{i=d+1}^m \binom{m}{i} a^i \\ &= L + U, \end{aligned} \quad (3)$$

where L and U are defined as follows

$$L := \sum_{i=0}^d \binom{m}{i} a^i = \sum_{i=0}^d \binom{m}{d-i} a^{d-i}, \quad \text{and} \quad (4)$$

$$U := \sum_{i=d+1}^m \binom{m}{i} a^i = \sum_{i=0}^d \binom{m}{d+i+1} a^{d+i+1}. \quad (5)$$

Now observe that L and U have the same number of summands with identical respective binomial coefficients, namely

$$\binom{m}{d-i} a^{d-i} \quad \text{and} \quad \binom{m}{d+i+1} a^{d+i+1},$$

for $i = 0, 1, \dots, d$. In Formulas (4)-(5) observe that the left term when multiplied by a^{2i+1} is equal to the right term, namely $a^{2i+1} \binom{m}{d-i} a^{d-i} = \binom{m}{d+i+1} a^{d+i+1}$, for $i = 0, 1, \dots, d$. Since $a > 1$ and $d \geq 1$ we conclude that

$$aL = \sum_{i=0}^d a \binom{m}{d-i} a^{d-i} < \sum_{i=0}^d a^{2i+1} \binom{m}{d-i} a^{d-i} = U. \quad (6)$$

From Equations (3) and (6), it follows that $(a+1)^m = L + U < \left(\frac{1}{a} + 1\right) U$. Since $a + 1 = \frac{1}{p}$, we conclude that

$$U > \frac{(a+1)^m}{\frac{1}{a} + 1} = \frac{1-p}{p^m}.$$

Case 2: m is even. The proof is similar to the case when m is odd. Since m is even it can be written as $m = 2d$, for some integer $d \geq 1$ so that $\lceil m/2 \rceil = d$. Let $a = \frac{1}{p} - 1$ and observe that $a > 1$, since $p < \frac{1}{2}$. From the binomial theorem we have that

$$\begin{aligned} (a+1)^m &= \sum_{i=0}^m \binom{m}{i} a^i \\ &= \sum_{i=0}^{d-1} \binom{m}{i} a^i + \sum_{i=d}^m \binom{m}{i} a^i \\ &= L' + U', \end{aligned} \quad (7)$$

where L' and U' are defined as follows

$$L' := \sum_{i=0}^{d-1} \binom{m}{i} a^i = \sum_{i=1}^d \binom{m}{d-i} a^{d-i}, \quad \text{and} \quad (8)$$

$$U' := \sum_{i=d}^m \binom{m}{i} a^i = \sum_{i=0}^d \binom{m}{d+i} a^{d+i}. \quad (9)$$

Now we compare summands in L' and U' , namely

$$\binom{m}{d-i} a^{d-i} \text{ and } \binom{m}{d+i} a^{d+i},$$

for $i = 0, 1, \dots, d$. In Formulas (8)-(9) observe that the left term when multiplied by a^{2i} is equal to the right term, namely $a^{2i} \binom{m}{d-i} a^{d-i} = \binom{m}{d+i} a^{d+i}$, for $i = 0, 1, \dots, d$. Since $a > 1$ and $d \geq 1$ we conclude that

$$aL' \leq \sum_{i=0}^d a \binom{m}{d-i} a^{d-i} < \sum_{i=0}^d a^{2i} \binom{m}{d-i} a^{d-i} = U'. \quad (10)$$

From Equations (7) and (10), it follows that $(a+1)^m = L + U < (\frac{1}{a} + 1)U$. Since $a+1 = \frac{1}{p}$, we conclude that

$$U' > \frac{(a+1)^m}{\frac{1}{a} + 1} = \frac{1-p}{p^m}.$$

Therefore, Inequality (2) is proved in both cases of m odd and m even. Thus, the proof of Lemma IV.1 is complete. \square

We may now conclude the following.

Theorem IV.2. *The majority rule applied to a swarm of m MAVs executing Algorithm 1 reduces the probability of error of the recognition process as long as p is less than $1/2$.*

Proof. Let m be the number of MAVs. Therefore $1 - p_m$ is the probability that the majority is at least composed of $\lceil m/2 \rceil$ MAVs correctly performing recognition, i.e.,

$$\begin{aligned} 1 - p_m &= \sum_{i=\lceil m/2 \rceil}^m \binom{m}{i} (1-p)^i p^{m-i} \\ &= p^m \sum_{i=\lceil m/2 \rceil}^m \binom{m}{i} \left(\frac{1}{p} - 1\right)^i. \end{aligned} \quad (11)$$

Now, for $p < 1/2$ Lemma IV.1 says that

$$1 - p < p^m \sum_{i=\lceil m/2 \rceil}^m \binom{m}{i} \left(\frac{1}{p} - 1\right)^i, \quad (12)$$

which in view of Equation (11) implies that $p_m < p$, i.e., the probability of error for a swarm of m MAVs is less than for MAV in solo. This proves the theorem. \square

A similar proof also yields the following.

Theorem IV.3. *The majority rule applied to a swarm of m MAVs executing Algorithm 2 reduces the probability of error of the advice process as long as $q < 1/2$,*

Proof. The proof is similar to the proof of Theorem IV.3. \square

Note that there are additional possibilities in Algorithm 2. The MAVs in a swarm could also acquire information either from the same landmark or from different landmarks (although we do not investigate the latter case further).

B. Approximating the majority

Let S_m be the sum of m mutually independent random variables each taking the value 1 with probability p and the value 0 with probability $1-p$ (i.e., Bernoulli random trials). The majority probability discussed above is given by the formula $\Pr[S_m \geq \lceil \frac{m}{2} \rceil]$. Good approximations of the majority probability for large values of m can be obtained from the central limit theorem which states that

$$\Pr \left[a \leq \frac{S_m - mp}{\sqrt{mp(1-p)}} \leq b \right] \rightarrow \frac{1}{\sqrt{2\pi}} \int_a^b e^{-x^2/2} dx. \text{ as } m \rightarrow \infty \quad (13)$$

(see e.g., [19]). For example, for any m we have that

$$S_m \geq \left\lceil \frac{m}{2} \right\rceil \Leftrightarrow \frac{S_m - mp}{\sqrt{mp(1-p)}} \geq \frac{\left\lceil \frac{m}{2} \right\rceil - mp}{\sqrt{mp(1-p)}}.$$

Hence, the central limit theorem (13) is applicable with $a = \frac{\lceil \frac{m}{2} \rceil - mp}{\sqrt{mp(1-p)}}$ and $b = +\infty$, where $p < 1/2$ is a constant..

V. EXPERIMENTS AND SIMULATIONS

There is an interesting tradeoff between the majority probability p_m and the cost of using a swarm of m MAVs. This might help us put the probabilistic gains in context w.r.t. the energy consumption and/or time costs of the swarm.

A. Cost measures and tradeoffs

We know that Theorem IV.2 reduces the error probability for any number m of MAV from p to p_m (similarly for Theorem IV.3). We now examine quantitative estimates of this reduction in error that depends on the number m of MAVs employed.

Observe from Equation (11), that we can derive the following identity concerning the ratio of improvement of the probability of correctness, namely

$$\frac{1 - p_m}{1 - p} = \sum_{i=\lceil m/2 \rceil}^m \binom{m}{i} (1-p)^{i-1} p^{m-i}. \quad (14)$$

In a way, one can think of the righthand side of Equation (14) as the ‘‘fractional gain’’ in the correctness probability (because we are employing a majority rule) that improves it from $1-p$ to $1-p_m$. In general, we would like on the one hand to ensure that $\frac{1-p_m}{1-p} > 1$ and on the other hand optimize the righthand side of Equation (14). Since we are also interested in applying the majority algorithms for a relatively small number of MAVs, we give precise estimates for $m = 2, 3, 4, 5, 6, 7$.

Theorem V.1. *Valid values for a fractional gain of $\frac{1-p_m}{1-p}$*

m	maximized for	max. value	m	maximized for	max. value
2	p=0.500	1.500	3	p=0.250	1.125
4	p=0.462	1.379	5	p=0.276	1.198
6	p=0.398	1.368	7	p=0.294	1.249

Proof. For $m = 2$ MAVs, we can show that the ratio $\frac{1-p_2}{1-p} = \frac{1-p^2}{1-p} = 1+p$ is maximized for $p = 1/2$ and its maximum value is $1 + 1/2 = 1.5$.

For $m = 3$, the ratio $\frac{1-p_3}{1-p}$ is maximized for $p = 1/4$ and its maximum value is $1 + 1/8 = 1.125$. Indeed, calculations

show that for $m = 3$ the righthand side of Equation (14) is equal to $1 + p - 2p^2$. Calculations also show that $1 + p - 2p^2$ is maximized when $p = 1/4$ and attains the maximum value $1 + 1/8$. Hence also $\frac{1-p_3}{1-p}$ is maximized when $p = 1/4$ and attains the maximum value $1 + 1/8 = 1.125$.

For $m = 4$, we have $\frac{1-p_4}{1-p} = (1-p)(3p^2 + 2p + 1)$, maximized for $p = \frac{1+\sqrt{10}}{9}$.

For $m = 5$, $\frac{1-p_5}{1-p} = 10(1-p)^2p^2 + 5(1-p)^3p + (1-p)^4$. The derivative of the righthand side with respect to p is equal to $24p^3 - 27p^2 + 2p + 1$. One of the roots of this polynomial is $p = 1$ and therefore $24p^3 - 27p^2 + 2p + 1 = (p-1)(24p^2 - 3p + 1)$. The positive root of the quadratic $24p^2 - 3p + 1$ is equal to $p = \frac{3+\sqrt{9+96}}{48} = \frac{3+\sqrt{105}}{48} \approx 0.275978$ and attains the maximum value 1.1917.

For $m = 6$, $\frac{1-p_6}{1-p} = (1-p)^2(20p^3 + 15(1-p)p^2 + 6(1-p)^2)p + (1-p)^3$. This is maximized for 1.368.

For $m = 7$, $\frac{1-p_7}{1-p} = (1-p)^3(35p^3 + 35(1-p)p^2 + 7(1-p)^2 \cdot p + (1-p)^3)$. The derivative of the righthand side above is $(1-p)^2(-42 \cdot p^3 - 102 \cdot p^2 + 32 \cdot p + 1)$ which yields the root $p \approx 0.294$ and attains the maximum value 1.249. \square

Table I displays the polynomials arising in the fractional gain for $m = 2, 3, \dots, 7$. The improvement provided in Theorem IV.2 is more substantial when the number m of MAVs gets larger. This is also confirmed by the calculations above. Table II displays the optimal error probability and fractional gain and the last column the majority error probability p_m for a given number m of MAVs, where $m \leq 21$. Figure 3 (a) plots the evaluation of equation $\frac{1-p_m}{1-p}$ from $m = 2$ to $m = 20$ and Figure 3 (b) from $m = 3$ to $m = 21$. The resulting curve indicates the maximum value of $\frac{1-p_m}{1-p}$ for p .

B. Numerical Simulations

Algorithms 1 and 2 have been integrated into a Java simulator, which implements swarm populations modeled as mobile agents. Each swarm executes the algorithms within a terrain of interconnected landmarks. It consists of a simple discrete event, time-step based simulation engine, in which the swarm executes our algorithms at every step of simulated time. The simulation engine implements a discrete event scheduler, a graphical view, a data collection system, and the simulated objects themselves, i.e., landmarks and agents.

TABLE I

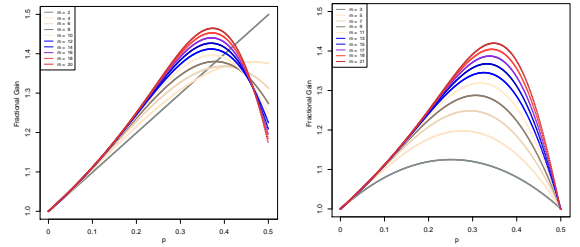
LEFT TO RIGHT COLUMNS PROVIDE (1) THE NUMBER OF MAVS, (2) THE ERROR PROBABILITY (p), (3) THE FRACTIONAL GAIN $\frac{1-p_m}{1-p}$ FROM $m = 2$ TO $m = 7$, AND (4) THE CORRESPONDING MAJORITY ERROR.

# MAVs	Optimal Error p	Fractional Gain $\frac{1-p_m}{1-p}$	Majority Error p_m
$m = 2$	0.500	1.500 $1 + p$	0.250
$m = 3$	0.250	1.125 $-2p^2 + p + 1$	0.156
$m = 4$	0.462	1.379 $-3p^3 + p^2 + p + 1$	0.257
$m = 5$	0.276	1.198 $6p^4 - 9p^3 + p^2 + p + 1$	0.133
$m = 6$	0.398	1.368 $10p^5 - 14p^4 + p^3 + p^2 + p + 1$	0.176
$m = 7$	0.294	1.249 $-20p^6 + 50p^5 - 34p^4 + p^3 + p^2 + p + 1$	0.118

TABLE II

LEFT TO RIGHT COLUMNS PROVIDE (1) THE NUMBER OF MAVS, (2) THE ERROR PROBABILITY (p), (3) THE FRACTIONAL GAIN $\frac{1-p_m}{1-p}$ FROM $M = 9$ TO $M = 21$, AND (4) THE CORRESPONDING MAJORITY ERROR.

# MAVs	Optimal Error p	Fractional Gain $\frac{1-p_m}{1-p}$	Majority Error p_m
$m = 9$	0.307	1.288	0.108
$m = 10$	0.372	1.396	0.123
$m = 11$	0.317	1.319	0.099
$m = 12$	0.370	1.411	0.110
$m = 13$	0.326	1.345	0.093
$m = 14$	0.370	1.426	0.101
$m = 15$	0.333	1.368	0.088
$m = 16$	0.371	1.440	0.094
$m = 17$	0.339	1.387	0.083
$m = 18$	0.373	1.452	0.089
$m = 19$	0.344	1.404	0.079
$m = 20$	0.374	1.464	0.083
$m = 21$	0.349	1.420	0.076



(a) Even numbers of MAVs (b) Odd number of MAVs

Fig. 3. Plots of the fractional gain function $\frac{1-p_m}{1-p}$ for varied p 's.

Further information about the numerical simulations is available in the Appendix of this paper. Videocaptures and source code are available online, at <http://j.mp/mavsim> and [GitHub](#).

VI. CONCLUSION

We have presented an error tolerant path planning algorithm for MAV swarms. We have assumed a navigation system for the swarm, in which the MAVs find their path by using their onboard cameras, by identifying and following a series of visual landmarks. We have assumed that the landmarks have a-priori information whose interpretation (by the MAVs) is error prone. We have defined two types of errors: (1) *recognition* errors (e.g., due to faulty sensors which misinterpret the sensed data) and (2) *advice* errors caused by the landmarks (e.g., due to weather conditions or outdated information). Our solution benefits from swarm cooperation. If the MAVs in the swarm can communicate and exchange information, the *recognition* and *advice* error ratios get minimized to one fourth with the cost of increasing the total number of MAVs by twenty. We have validated our proposal with appropriate simulations, implemented over a Java simulator available at <http://j.mp/mavsim> and [GitHub](#).

The recognition and advice algorithms presented are based on binary decision making. An interesting setting worth exploring is non-binary. For example, consider a swarm of five MAVs required to decide for its next move based on the majority color of a door (say, among Yellow (Y), Green (G), Blue (B)); in this case it is assumed that Y is to be positive outcome while G, B negative outcomes. On the one hand, if the respective outputs of the visual systems are Y, G, Y, Y,

B then Yellow Door is considered to be the positive outcome and occurs three out of five times. On the other hand if the respective outputs of the visual systems are Y, G, Y, B, B than there is no majority of identical colors. In particular, majority can be formed by three identical answers. Such situations can be handled using voting schemes and fuzzy logic, which would be the focus of future research.

The basic idea of our algorithms is to enhance quality of recognition and advice by having multiple MAVs make a decision after exchanging the information they have obtained. Naturally, this increases the cost of movement since multiple MAVs will be travelling to a destination. Therefore it would be interesting to look at trade-offs of the cost of the search that take into account either time or total energy versus the number of MAVs in the swarm for a given cost budget.

Acknowledgments — Research supported in part by NSERC Discovery grant, and the European Commission under grant agreement 830892 (H2020 SPARTA project).

REFERENCES

- [1] Aerial Robots for Sewer Inspection, “ARSI,” Last Access: 2019, available at http://echord.eu/essential_grid/arsi/.
- [2] Altigator, “Drones for search and rescue missions,” Last Access: 2019, available at <https://altigator.com/drones-for-search-rescue-missions/>.
- [3] DHL, “DHL’s Parcelcopter: changing shipping forever,” Last Access: 2019, available at <http://bit.ly/2WV7KcO>.
- [4] C. Goerzen, Z. Kong, and B. Mettler, “A survey of motion planning algorithms from the perspective of autonomous uav guidance,” *Journal of Intelligent and Robotic Systems*, vol. 57, no. 1-4, p. 65, 2010.
- [5] M. Radmanesh, M. Kumar, P. H. Guentert, and M. Sarim, “Overview of path-planning and obstacle avoidance algorithms for uavs: A comparative study,” *Unmanned Systems*, vol. 06, no. 02, pp. 95–118, 2018.
- [6] O. Khatib, “Real-time obstacle avoidance for manipulators and mobile robots,” *The International Journal of Robotics Research*, vol. 5, no. 1, pp. 90–98, 1986.
- [7] S. M. LaValle, “Rapidly-exploring random trees: A new tool for path planning,” Department of Computer Science, Iowa State University, Tech. Rep., 1998.
- [8] S. LaValle, *Planning Algorithms*. Cambridge University Press, 2006.
- [9] M. Turpin, N. Michael, and V. Kumar, “CAPT: Concurrent assignment and planning of trajectories for multiple robots,” *The International Journal of Robotics Research*, vol. 33, no. 1, pp. 98–112, 2014.
- [10] A. A. A. Rizqi, A. I. Cahyadi, and T. B. Adji, “Path planning and formation control via potential function for uav quadrotor,” in *2014 International Conference on Advanced Robotics and Intelligent Systems (ARIS)*. IEEE, 2014, pp. 165–170.
- [11] D. Maravall, J. de Lope, and J. Fuentes, “Navigation and self-semantic location of drones in indoor environments by combining the visual bug algorithm and entropy-based vision,” *Frontiers in neurorobotics*, vol. 11, p. 46, 2017.
- [12] A. Weinstein, A. Cho, G. Loianno, and V. Kumar, “Visual inertial odometry swarm: An autonomous swarm of vision-based quadrotors,” *IEEE Robotics and Automation Letters*, vol. 3, no. 3, pp. 1801–1807, 2018.
- [13] D. Maravall, J. de Lope, and J. P. F. Brea, “A vision-based dual anticipatory/reactive control architecture for indoor navigation of an unmanned aerial vehicle using visual topological maps,” in *International Work-Conference on the Interplay Between Natural and Artificial Computation*. Springer, 2013, pp. 66–72.
- [14] K. Narendra and M. Thathachar, *Learning automata: an introduction*. Courier Corporation, 2012.
- [15] D. Maravall, J. De Lope, and J. P. Fuentes, “Fusion of probabilistic knowledge-based classification rules and learning automata for automatic recognition of digital images,” *Pattern Recognition Letters*, vol. 34, no. 14, pp. 1719–1724, 2013.
- [16] J. P. Fuentes, D. Maravall, and J. de Lope, “Entropy-based search combined with a dual feedforward-feedback controller for landmark search and detection for the navigation of a uav using visual topological maps,” in *ROBOT2013: First Iberian Robotics Conference*. Springer, 2014, pp. 65–76.
- [17] E. Kranakis and D. Krizanc, “Searching with uncertainty,” in *SIROCCO’99, 6th International Colloquium on Structural Information & Communication Complexity, Lacanau-Ocean, France, 1-3 July, 1999, 1999*, pp. 194–203.
- [18] L. M. Kirousis, E. Kranakis, D. Krizanc, and Y. C. Stamatiou, “Locating information with uncertainty in fully interconnected networks,” in *International Symposium on Distributed Computing*. Springer, 2000, pp. 283–296.
- [19] Y. A. Rozanov, *Probability theory: a concise course*. Dover, 1977.
- [20] W. Shi, J. Garcia-Alfaro, and J.-P. Corribeau, “Searching for a black hole in interconnected networks using mobile agents and tokens,” *Journal of Parallel and Distributed Computing*, vol. 74, no. 1, pp. 1945–1958, 2014.
- [21] T. Cormen, C. Leiserson, R. Rivest, and C. Stein, *Introduction to algorithms*. MIT press, 2009.
- [22] C. Di Franco and G. Buttazzo, “Energy-aware coverage path planning of uavs,” in *2015 IEEE International Conference on Autonomous Robot Systems and Competitions*. IEEE, 2015, pp. 111–117.

Appendix A. This technical appendix reports the use of the MAVs Java simulator (MAVSIM, cf. <http://j.mp/mavsim>) and reports the experimental results associated to Section V.B (Numerical Simulations).

A.1 GENERATION OF NEW MAPS AND LANDMARKS

In addition to the topological structures of the simulator already reported in [20] (including random graphs, grids, hypercubes, and tori, cf. <http://j.mp/scavesim> for further details), MAVSIM has been extended to include as well the topological structures associated to the path planning algorithms for MAVs presented in this paper. This includes topological structures associated to blueprints of existing cities, as well as structures from geographical terrains, complemented by *smart landmarks* providing advice to the swarm of MAVs. In this section, we show how to generate the new topological structures of MAVSIM exporting data from the [OpenStreetMap](http://www.openstreetmap.org) online service (i.e., exporting and transforming the OSM files from *OpenStreetMap* into the internal structures of MAVSIM).

To use the new functionality of the simulator, the following items have been added to the list of resources associated to the simulator available at [GitHub/scavesim-mavsim](https://github.com/scavesim-mavsim). The source code and the associated files are all available online, at the aforementioned link, as well as in the companion website, under the *github entry* listed in <http://j.mp/mavsimTechRep>.

- **./ci.py**: Makes the confidence intervals and plots the results.
- **./energy_consumption.py**: Plots the energy consumption.
- **./simu.sh**: Command to run the simulation several times.
- **./scenario**: Folder to save the generated scenarios (**do not remove it**)
- **./results**: Folder to save the results for each simulation.
- **./python.py**: Python code to convert OSM files (cf. [OpenStreetMap](http://www.openstreetmap.org)) to the simulator internal structures.

In order to generate the new maps and the series of smart landmarks reported in this paper, follow the instructions below.

- 1) Go to <https://www.openstreetmap.org/>.
- 2) In the “Search” section, type a place (e.g., *Carleton University*).
- 3) Go to the “Export” section, select “Select another area manually”, then “Export”.

- 4) Transform the obtained files, as follows:

```
ant poly -DinputNet="scenario.net.xml" \
-DinputOSM="scenario.osm" \ \
-Doutput="scenario.poly.xml"
```

- 5) The file “scenario.poly.xml” contains the geometrical shapes (polygons or points of interest) that can be visualized using the [SUMO-GUI](#) toolkit. As an example, you can test the following:

```
ant poly -DinputNet="paris.net.xml" \ \
-DinputOSM="paris.osm" \ \
-Doutput="paris.poly.xml"
```

```
ant python -DinputNet="paris.net.xml" \ \
-DinputPoly="paris.poly.xml"
```

```
[exec] Number of Nodes: 1469
```

```
[exec] Number of Landmarks: 97
```

```
[exec] Type of landmarks set(['highway.traffic
signals', 'highway.motorway_junction', 'highway
.turning_circle', 'highway.crossing', 'tourism
.viewpoint', 'amenity.parking',
'highway.elevator'])
```

```
[echo] Generated files: edges_paris.txt
and vertices_paris.txt.
```

```
BUILD SUCCESSFUL
```

```
Total time: 36 seconds
```

- 6) The execution of the previous example generates a simulator scenario which contains 1469 nodes and 97 landmarks (i.e., 'highway.traffic_signals', 'highway.motorway_junction', 'highway.turning_circle', 'highway.crossing', 'tourism.viewpoint', 'amenity.parking', 'highway.elevator'). Notice that it is possible to generate landmarks as traffic_signals, crossing, tourism viewpoint, bicycle parking, stop signal, tree, cinema, library, etc.

- 7) In order to run some experimental simulations using MAVSIM and the series of landmarks explained before, type the following:

```
ant run -Dagents=1 \ \
-Dedges="edges_paris.txt" \ \
-Dvertices="vertices_paris.txt" \ \
-Doutfile="paris.txt" \ \
-DagentSize=0.003 \ \
-DnodeSize=0.001 \ \
-DminLandmarks=97
```

Note that the `-DminLandmarks=X` option fixes a minimum number of landmarks to cross by the

swarm of MAVs. The [Floyd-Warshall Algorithm](#) [21] is used by MAVSIM to find the shortest distances between every pair of landmarks. To decrease the simulation time, the shortest path is stored as `MavSim/results/path.txt`.

A.2 EXPERIMENTAL RESULTS

We validate the solution presented in this paper with five different scenarios. Each scenario relates the number of MAVs with the error probability of the majority rule varying the *recognition* and *advice* error ratios between 70%, 80%, and 90% (cf. Section III).

Figures 4(a,b) represent two traditional grid structures of MAVSIM (i.e., a 10×10 -grid and a 25×25 -grid). Figures 4(c,d,e) represent three additional structures exported using the [OpenStreetMap](#) online service. More precisely:

- Figure 4(a) shows a 10×10 -grid structure of MAVSIM.
- Figure 4(b) a 25×25 -grid structure.
- Figure 4(c) a topological structure exported from *OpenStreetMap* using *Carleton University* as location.
- Figure 4(d) a topological structure exported from *OpenStreetMap* using Telecom SudParis (at the NanoInnov center of the campus of the Institut Polytechnique de Paris (IPP) and the Paris-Saclay University) as location.
- Figure 4(e) a topological structure exported from *OpenStreetMap* using University of Campinas – Unicamp as location.

A. Performance Evaluation

Table III shows some representative characteristics of each of the previous scenarios. Figure 5 shows the relation between the number of MAVs and the error probability of the majority rule varying the *recognition* and *advice* error ratios between 70%, 80%, and 90% using, respectively, the 10×10 -grid, 25×25 -grid, Carleton, Telecom SudParis, and Unicamp scenarios. The results in Figure 5 also show that the majority rule applied to a swarm of m MAVs reduces the probability of error of the recognition process and our solution benefits from swarm cooperation.

B. Energy Evaluation

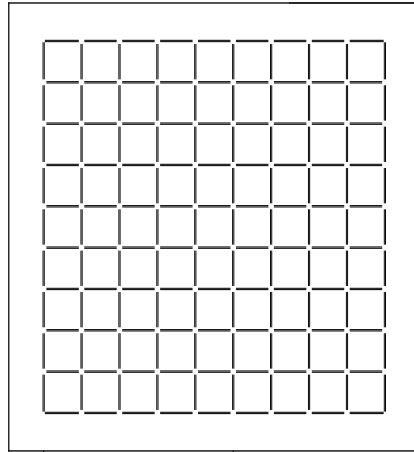
The energy consumed in a straight flight E_{fly} to move a distance d at a given speed s_i can be computed as the integral of the power $P(s_i)$ in function of the given speed s_i along the time [22]:

$$E_{fly}(d, s_i) = \int_{t=0}^{t=d/s_i} P(s_i) dt = P(s_i) \frac{d}{s_i} \quad (15)$$

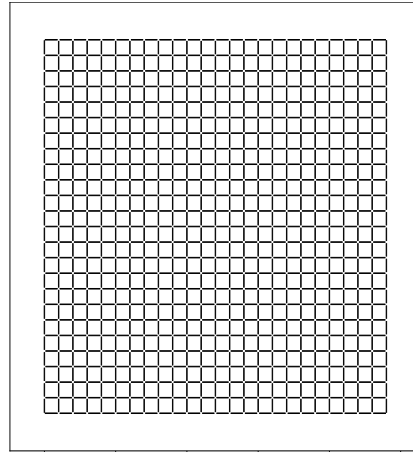
Figure 6 shows the relating the number of MAVs and the energy consumption varying the *recognition* and *advice* error ratios between 70%, 80%, and 90% in the aforementioned scenarios (10×10 -grid, 25×25 -grid, Carleton University, Telecom SudParis, and Unicamp, respectively). The results show that the energy consumption of the MAVs reduces to approximately 35% when the number of MAVs increases.

TABLE III
CHARACTERISTICS OF EACH SCENARIO

Scenario	Landmark types	# of nodes	# of landmarks
10 × 10-grid	Random nodes	100	1/4 of the nodes
25 × 25-grid	Random nodes	625	1/4 of the nodes
Carleton University	Traffic signals, junctions, etc.	3511	335
IPP – Telecom SudParis	Crossing paths, tourism viewpoint, etc.	1413	97
Campinas – Unicamp	Crossing paths, round-about, etc.	1559	29



(a) 10 × 10-grid



(b) 25 × 25-grid



(c) Carleton University



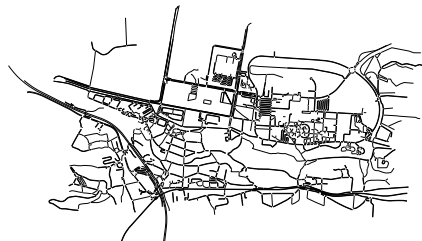
(d) IPP – T. SudParis



(e) Campinas – Unicamp



(f) Carleton University Map



(g) IPP – T. SudParis Map



(h) Campinas – Unicamp Map

Fig. 4. Sample MAVSIM scenarios for the experimental results.

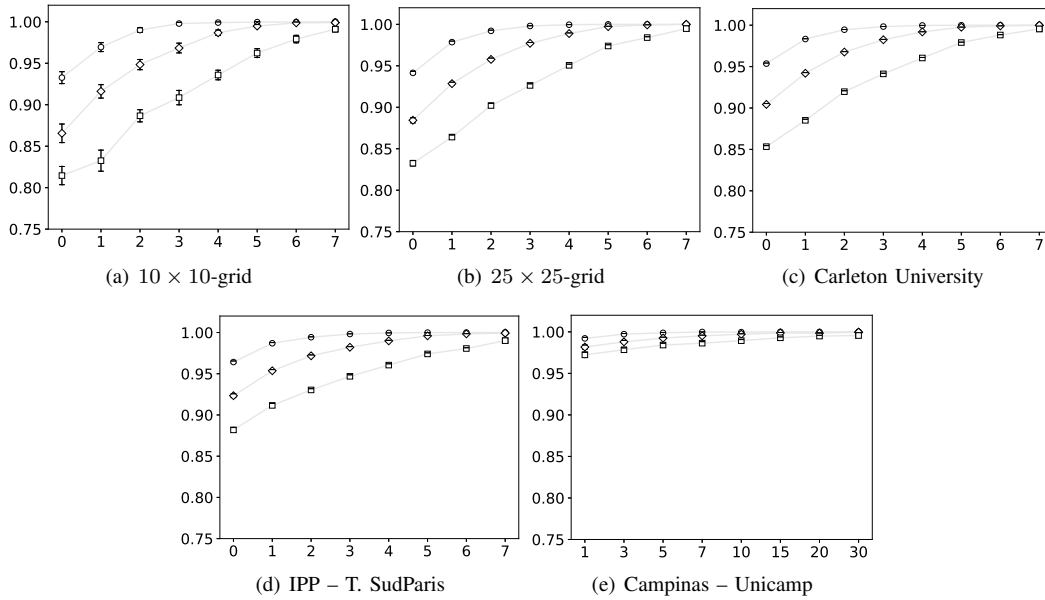


Fig. 5. Relation between the number of MAVs and the error probability of the majority rule varying the *recognition* and *advice* error ratios between 70% (squares), 80% (diamonds), and 90% (circles). The vertical axis represents the error probability. The horizontal axis represents the number of MAVs.

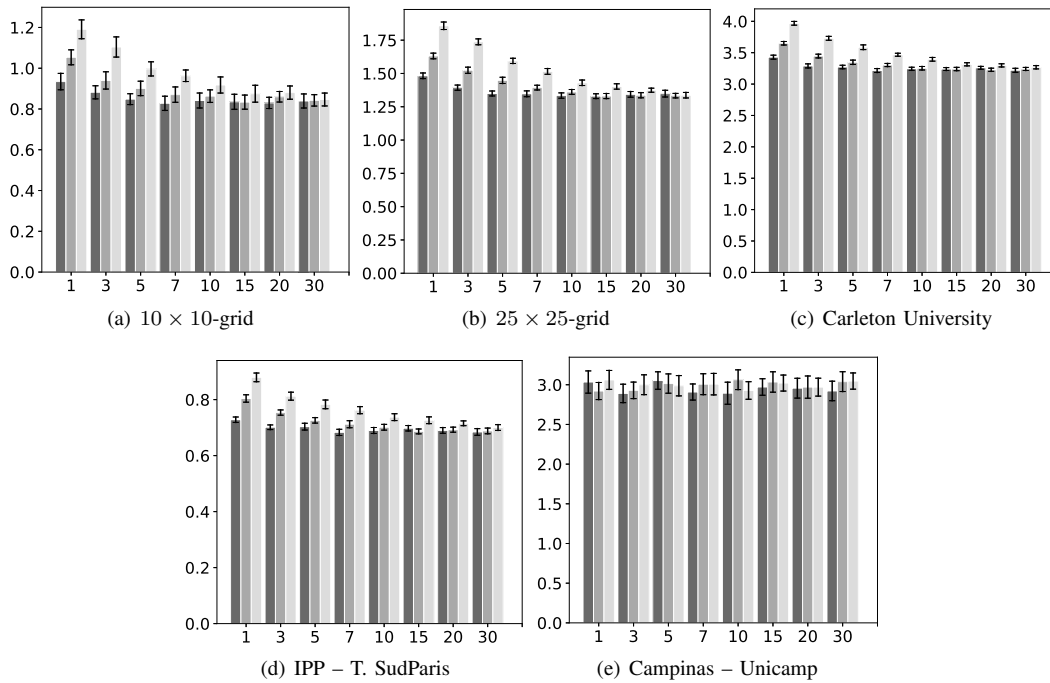


Fig. 6. Relation between the number of MAVs vs. energy consumption, when varying the *recognition* and *advice* error ratios from 70% (light-gray), to 80% (gray) and 90% (dark-gray), and $s_i = 5$ m/s. The vertical axis represents the energy consumption (joules). The horizontal axis represents the number of MAVs.